Biological Psychiatry: GOS

Archival Report

Postnatal Phencyclidine-Induced Deficits in Decision Making Are Ameliorated by Optogenetic Inhibition of Ventromedial Orbitofrontal Cortical Glutamate Neurons

Michael M. Tranter, Lauren Faget, Thomas S. Hnasko, Susan B. Powell, Daniel G. Dillon, and Samuel A. Barnes

ABSTRACT

BACKGROUND: The orbitofrontal cortex (OFC) is essential for decision making, and functional disruptions within the OFC are evident in schizophrenia. Postnatal phencyclidine (PCP) administration in rats is a neurodevelopmental manipulation that induces schizophrenia-relevant cognitive impairments. We aimed to determine whether manipulating OFC glutamate cell activity could ameliorate postnatal PCP-induced deficits in decision making.

METHODS: Male and female Wistar rats (n = 110) were administered saline or PCP on postnatal days 7, 9, and 11. In adulthood, we expressed YFP (yellow fluorescent protein) (control), ChR2 (channelrhodopsin-2) (activation), or eNpHR 3.0 (enhanced halorhodopsin) (inhibition) in glutamate neurons within the ventromedial OFC (vmOFC). Rats were tested on the probabilistic reversal learning task once daily for 20 days while we manipulated the activity of vmOFC glutamate cells. Behavioral performance was analyzed using a Q-learning computational model of reinforcement learning.

RESULTS: Compared with saline-treated rats expressing YFP, PCP-treated rats expressing YFP completed fewer reversals, made fewer win-stay responses, and had lower learning rates. We induced similar performance impairments in saline-treated rats by activating vmOFC glutamate cells (ChR2). Strikingly, PCP-induced performance deficits were ameliorated when the activity of vmOFC glutamate cells was inhibited (halorhodopsin).

CONCLUSIONS: Postnatal PCP-induced deficits in decision making are associated with hyperactivity of vmOFC glutamate cells. Thus, normalizing vmOFC activity may represent a potential therapeutic target for decision-making deficits in patients with schizophrenia.

https://doi.org/10.1016/j.bpsgos.2023.08.002

Making optimal decisions involves learning from past experiences and modifying behavior when the environment changes. Several psychiatric and neurological disorders, including schizophrenia, mood disorders, obsessive-compulsive disorder, Parkinson's disease, and substance use disorder, are associated with deficits in learning and decision making (1–8). Because decision-making deficits contribute to poor patient outcomes (9), a better understanding of the underlying pathophysiology would facilitate the development of more effective treatments.

Decision-making deficits in schizophrenia can be measured using a probabilistic reversal learning (PRL) task, which requires subjects to discriminate between more versus less frequently rewarded stimuli and adjust their behavior when the reinforcement contingencies reverse (10,11). In several studies, patients with schizophrenia completed fewer reversals than healthy control participants and exhibited impairments during both the initial discrimination and the reversal phase after the contingencies switched (1–3). Assessing win-stay (repeating a choice after reward receipt) and lose-shift (choosing the alternative stimulus after no reward) responding can provide insight into whether such behavioral deficits reflect abnormal reward versus loss sensitivity (12,13). Robust impairments in win-stay behavior are evident in schizophrenia (1,2), indicating that reduced reward sensitivity contributes to excessive switching between stimuli and poorer PRL performance overall (14).

The difficulty in using trial-by-trial information to guide decisions that is evident in schizophrenia may reflect dysfunction in the orbitofrontal cortex (OFC) (15). Indeed, structural and functional abnormalities in the OFC are evident in people with schizophrenia (16–18). While the underlying pathophysiology of schizophrenia is complex and encompasses multiple brain regions and neurotransmitter systems, deficits in cortical GABAergic (gamma-aminobutyric acidergic) interneurons are consistently seen in postmortem tissue from patients with schizophrenia (19–21). Because GABAergic interneurons provide critical inhibitory control over excitatory pyramidal

SEE COMMENTARY ON PAGE 103

ISSN: 2667-1743

neurons (22,23), these abnormalities may contribute to functional hyperactivation of the OFC that has been reported in schizophrenia (24–26). Given the importance of the OFC in decision making, difficulty regulating excitatory neurotransmission in this brain region may contribute to impaired decision making in patients with schizophrenia.

Rodent versions of the PRL task enable careful investigation of the neural mechanisms underlying task performance with greater precision than is currently possible with humans. One hypothesis is that schizophrenia has neurodevelopmental origins (27,28) that result from dysfunctional glutamatergic transmission (29). Along these lines, administering the NMDA receptor (NMDAR) antagonist phencyclidine (PCP) to rodents during early postnatal neurodevelopment is commonly used to induce long-lasting cognitive deficits and pathophysiological abnormalities associated with schizophrenia (30–32). For example, postnatal PCP treatment impairs executive functioning (33,34), sociability (35), and spatial (36) or working memory (37). Furthermore, we recently reported that postnatal PCP-treated rats exhibited impaired PRL performance (38). Consistent with PRL deficits seen in schizophrenia, these PCP-induced deficits reflected a low learning rate and difficulty using trial-by-trial information to guide behavior. Postnatal PCP-treated rats also exhibit functional abnormalities in cortical GABAergic interneurons that diminish their ability to inhibit excitatory pyramidal cells (39–41). We recently showed that hyperactivation of ventromedial OFC (vmOFC) glutamate neurons was associated with disrupted PRL performance resulting from reduced reward sensitivity (42). Thus, we infer that impaired PRL performance in postnatal PCP-treated rats may result from disinhibition or hyperactivity of vmOFC glutamatergic neurons. Therefore, the current study tested the hypotheses that 1) PCP-induced impairments in PRL can be replicated in saline-treated control rats by hyperactivating vmOFC glutamate neurons, and 2) PCP-induced PRL impairments can be ameliorated by inhibiting vmOFC glutamate neurons.

METHODS AND MATERIALS

Animals

Timed-pregnant Wistar dams (Charles River Laboratories) were obtained on day 13 of gestation. Dams were housed individually in a climate-controlled room on a reverse 12-hour light cycle (lights off at 07:00 AM) with ad libitum access to food and water. Male and female pups were randomly assigned to litters of 8 (4 pups per sex) and cross-fostered between dams. All procedures followed guidelines from the National Institutes of Health and the Association for Assessment and Accreditation of Laboratory Animal Care and were approved by the University of California, San Diego Institutional Animal Care and Use Committee.

Drug Treatment

As previously described (38,40,43), pups were subcutaneously administered vehicle (0.9% saline) or PCP (20 mg/kg) on postnatal days (PNDs) 7, 9, and 11. Representatives from each treatment group were present in each litter. Pups were weaned on PND 21, split by sex, and group housed until 4 to 5 weeks of age, after which they were housed in pairs of the same sex and treatment group. Behavioral testing began after PND 60.

Apparatus

Behavioral training and testing were conducted in 9-hole operant boxes (Med Associates) contained within light- and sound-attenuating chambers (38). Briefly, the rear wall was a curved array with 5 open response apertures. Throughout training and testing, only apertures 2 and 4 were active. A 3W stimulus light located at the aperture rear provided visual stimuli. On the opposite wall, a receptacle delivered food rewards (45 mg sucrose pellets, test diet; 5TUT). The apparatus was controlled by a personal computer running MedPC software (Med Associates).

Probabilistic Reversal Learning

PRL training was conducted as previously described (38). Once the criterion during the basic training session was met (≥90 responses for 2 consecutive days), PRL testing commenced. During PRL testing, rats were shown 2 illuminated apertures: one was the target location, and the other was the nontarget. Target responses were rewarded with 80% probability, while nontarget responses were rewarded with 20% probability (Figure 1A). A 2-second intertrial interval separated the trials, and responses during the intertrial interval resulted in a timeout. Once a rat made 8 consecutive target responses, the contingencies switched, with the nontarget becoming the target and vice versa. Reversals continued throughout the session each time the rat made 8 consecutive target responses. Sessions ended after 300 trials or 60 minutes, whichever came first. Rats were tested once daily for 20 days. Performance was assessed by determining the number of reversals completed per 100 trials. Win-stay responding was calculated as the percentage of trials during which the rat repeated a choice after being rewarded on the preceding trial. Lose-shift responding was calculated as the percentage of trials during which the rat switched responses after a reward was withheld on the preceding trial.

Computational Modeling

To investigate mechanisms that drive behavior, we analyzed the PRL data using a Q-learning model that is sensitive to PCP-induced performance deficits (38). Briefly, on each trial (t), the decision (i.e., which action to select) is likely guided by the value (Q) assigned to each action. Action values are updated according to whether a reward was delivered or not (r; reward = 1, no reward = 0) on each trial. Q values were initialized to 0.5 (neither good nor bad), and prediction errors (PEs) were calculated as follows:

$$PE = r_{(t)} - Q_{c(t)} \quad (1)$$

The PE served to update the value estimate of the chosen action on a given trial (Q_c) according to the equation below.

$$Qc_{(t+1)} = Qc + \alpha \times PE \quad (2)$$

In equation 2, the rate at which PEs updated value estimates was controlled by the learning rate (α). To simulate forgetting,

the rate at which the value of the unchosen action decayed was controlled by a forget parameter.

$$Qnc_{(t+1)} = (1 - forget) \times Qnc \quad (3)$$

Action values were converted into choice probabilities using the softmax function.

$$p(A) = \frac{e^{QA \times \beta}}{e^{QA \times \beta} + e^{QB \times \beta}} \quad (4)$$

The inverse temperature parameter (β) in the softmax equation controls the degree to which the subject chooses the higher-valued action (exploit; higher β values) or selects an action with an unknown or lower value (explore; lower β values). Although many other models of PRL performance are possible, this model successfully captured PCP-induced performance deficits in our previous work (38), and it is similar to models that are widely used in reinforcement learning.

To explore whether a difference in the sensitivity to rewards versus nonrewards was present in our experimental groups, we also implemented a model with separate learning rates for each outcome, as follows:

$$Qc_{(t+1)} = Qc + \alpha g \times PE \; if \; reward = 1 \quad (5)$$

$$Qc_{(t+1)} = Qc + \alpha l \times PE \; if \; reward = 0 \quad (6)$$

If the response resulted in a reward, then the rate at which PEs updated value estimates was controlled by the positive learning rate (α-gain; equation 5). However, for nonrewarded trials, the rate at which the PE updated value estimates was regulated by the negative learning rate (α-loss; equation 6). The value for the unchosen action was decayed using the same forgetting parameter described in equation 3, and action selection was controlled by the same softmax function described in equation 4.

For both models, the optimal parameter values for each subject were identified by minimizing the negative log-likelihood of choice probabilities using the minimize optimization function with the truncated Newton algorithm in Python's Scipy library (version 1.5). To sample broadly from the range of possible parameter values, and to reduce the possibility of the model getting stuck in local minima, the optimization algorithm was initialized with random starting points within the parameter space 15 times per dataset. The parameter values associated with the lowest negative log-likelihood were selected as the best-fitting values. The best-fitting model was identified by comparing the Bayesian information criterion values. To assess the quality of the chosen model, we conducted posterior predictive checks (38,44) and compared simulated data, generated using the best-fitting parameters, with the actual rodent data.

Optogenetics

Optogenetic stimulation was provided by six 473-nm diode pumped solid state 150 to 200 mW 3% stability lasers or six 532-nm diode pumped solid state 200 mW 1% stability lasers, each fitted with FC fiber couplers (OEM Lasers). Patch cables (200-μm core, 0.22 numerical aperture [NA] multimode fiber with 2.0-mm furcation tubing; Thorlabs) delivered light to 1 × 2 optical commutators (FRJ_1x2i_FC_2FC; Doric Lenses) fixed to a balance arm above the operant chamber. Custom-made patch cables (same specifications as above, with ferrule connector physical contact) connector to 2.5-mm ceramic ferrule with protective flexible metal jackets) delivered light to fiber implants. Output power was calibrated with a digital power meter (PM100D and S121C; Thorlabs) to 10 to 15 mW at the fiber tip. Optical stimulation (473 nm: 15-ms pulse width, 20 Hz for 2 seconds; 532 nm: continuous, 2 seconds) was controlled by Arduino Uno microcontrollers. Lasers were triggered by transistor-transistor-logic signals (SG-231; Med Associates) generated by action selection.

Surgical Procedures

Rats were anesthetized using isoflurane (1%–3%) and secured to a stereotaxic frame (David Kopf Instruments). The skull was exposed and cleaned using aseptic techniques. The skull was flat (incisor bar at −3.3 mm, the difference between DV coordinate at bregma and lambda ≤0.1 mm). AAV5-CaMKIIa-ChR2-eYFP (ChR2 [channelrhodopsin-2]), AAV5-CaMKIIa-eNpHR3.0-eYFP (halo [halorhodopsin]), or AAV5-CaMKIIa-eYFP (YFP [yellow fluorescent protein]) (titer 4.6–5.1 × 10^{12}; University of North Carolina Vector Core) was injected bilaterally into the vmOFC (anteroposterior + 4.2 mm, mediolateral ± 2.0 mm, dorsoventral −4.8 mm, 18° angle) at a flow rate of 0.1 μL/min for 7 minutes. The microinjector was left in place for 10 minutes and then slowly retracted. Optical fibers (200-μm core diameter, 0.37 NA, 2.5-mm ceramic ferrule; constructed with materials from Thorlabs) were implanted (same coordinates as above but dorsoventral −4.4 mm) and held in place with Geristore cement (Denmat) and covered with dental acrylic. Operant training resumed after at least 3 weeks to allow for adequate transgene expression.

Immunohistochemistry

After behavioral testing, rats were deeply anesthetized with sodium pentobarbital and transcardially perfused with ∼100 mL of saline followed by ∼200 mL 4% paraformaldehyde. Brains were extracted, postfixed in 4% paraformaldehyde at 4 °C for 48 hours, and transferred to 30% sucrose in phosphate-buffered saline (PBS) for >92 hours at 4 °C. Brains were frozen in isopentane and stored at −80 °C. For virus expression and optic fiber implant site verification, 30-μm coronal cryosections were cut using a cryostat (Leica CM 1860) and collected in PBS containing 0.01% sodium azide. For transgene signal amplification, brain sections were gently rocked 3 × 5 minutes in PBS containing 0.2% triton X-100 and blocked with 4% normal donkey serum in PBS containing 0.2% triton X-100 for 1 hour at room temperature. Sections were then incubated with rabbit anti–green fluorescent protein, 1:2000, Invitrogen A11122, in block at 4 °C overnight. Sections were rinsed 3 × 10 minutes with PBS containing 0.2% triton X-100 and incubated in donkey antirabbit secondary antibodies (711-545-152, Jackson ImmunoResearch) conjugated to Alexa488 fluorescent dye (2.5 μg/mL) for 2 hours at room temperature. Sections were then washed 3 × 10 minutes with

PBS, mounted, and coverslipped with Fluoromount-G mounting medium (Southern Biotech) ± DAPI (Roche, 0.5 μg/mL). Transgene expression was determined by epifluorescence microscopy using a Zeiss AxioObserver Z1 widefield epifluorescence microscope (10 × 0.45 NA, or 63 × 1.4 NA objective) and Zen blue software. High-magnification display images were acquired with a Zeiss ApoTome 2.0 for structured illumination.

Experimental Design

Postnatal saline- and PCP-treated rats underwent stereotaxic surgery to implant optic fibers and express YFP (control), ChR2 (neural excitation), or halo (neural inhibition) in glutamatergic neurons of the vmOFC (Figure 1B). After recovery, rats were trained to nose-poke response apertures for rewards and were habituated to fiber tethering. Once trained and habituated and after at least 3 weeks had elapsed (allowing sufficient time for transgene expression), rats were tested on the PRL task daily for 20 days. Optogenetic manipulation was triggered when the rat made its choice and nose-poked the response aperture. Consistent with our previous study (42), 2-second photostimulation was delivered on trials that yielded informative feedback (i.e., target responses that were rewarded and nontarget responses that were not rewarded) and triggered by the nose-poke response. Optogenetic stimulation was delivered during each session throughout the 20-day testing period.

Statistical Analysis

Performance on the PRL task was analyzed using four-way repeated-measures analyses of variance (ANOVAs) that included treatment, opsin, and sex as between-subject factors and day as the within-subject factor. When appropriate, significant interactions underwent post hoc adjustment using Fisher's least significant difference correction for multiple comparisons. p Values of $<.05$ were considered significant. Statistical analysis was conducted using R. Data are presented as mean ± SEM and graphically displayed using GraphPad Prism software.

RESULTS

The number of completed reversals increased across days ($F_{19,1862} = 115.43$, $p < .001$), demonstrating that performance improved with training in saline- and PCP-treated rats (Figure 1C). Additionally, we observed a treatment × opsin interaction ($F_{2,98} = 4.52$, $p < .05$). As shown in Figure 1D, this effect was driven by fewer completed reversals in YFP-expressing PCP-treated rats versus YFP-expressing saline-treated rats (Figure 1D, left), demonstrating that postnatal PCP

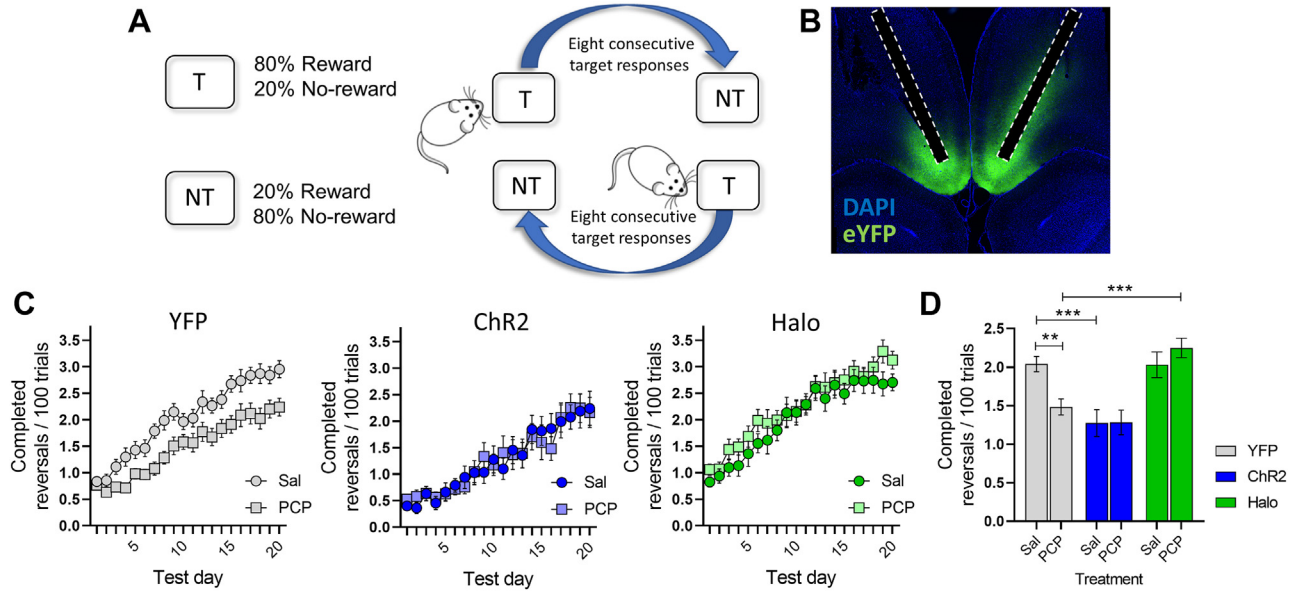

Figure 1. Effect of manipulating ventromedial orbitofrontal cortex glutamate cell activity during probabilistic reversal learning performance. The probabilistic reversal learning task requires the animal to discriminate between the target and nontarget stimuli. Responses are probabilistically reinforced (80:20 ratio), and the location of the target stimulus switches after 8 consecutive target responses **(A)**. An adeno-associated virus with a CaMKIIa promoter expressing either ChR2, halo, or YFP was injected bilaterally in the ventromedial orbitofrontal cortex, and optic fibers were implanted **(B)**. Rats were tested on the probabilistic reversal learning task once a day for 20 days. In both treatment groups (saline, PCP) and 3 opsin groups (YFP, ChR2, halo), the number of completed reversals increased across the 20-day testing period **(C)**. A between-group difference emerged for rats expressing YFP, with fewer completed reversals in PCP-treated than in saline-treated rats. Within the saline-treated group, rats expressing ChR2 completed fewer reversals than rats expressing YFP. Within the PCP-treated group, the number of reversals was increased in rats expressing halo vs. YFP **(D)**. Circles indicate saline-treated rats. Squares indicate PCP-treated rats. Gray color indicates YFP-expressing rats, blue indicates ChR2-expressing rats, green indicates halo-expressing rats. Saline YFP, $n = 11$ male, $n = 10$ female; saline ChR2, $n = 7$ male, $n = 8$ female; saline halo, $n = 9$ male, $n = 9$ female; PCP YFP, $n = 11$ male, $n = 10$ female; PCP ChR2, $n = 9$ male, $n = 7$ female; PCP halo, $n = 9$ male, $n = 10$ female. Data are presented as mean ± SEM. $^{**}p < .01$, $^{***}p < .001$. CamKIIa, calcium/calmodulin-dependent protein kinase IIa; ChR2, channelrhodopsin-2; eYFP, enhanced YFP; halo, halorhodopsin; NT, nontarget; PCP, phencyclidine; Sal, saline; T, target; YFP, yellow fluorescent protein.

treatment impaired PRL performance. Moreover, in saline-treated rats, activation of vmOFC glutamate cells by stimulating ChR2 replicated the reduction in reversals seen in PCP-treated rats (Figure 1D, center). By contrast, inhibition of vmOFC glutamate cells by stimulating halo ameliorated the PCP-induced deficit in reversals (Figure 1D, right). Analysis of the number of trials required to complete the initial discrimination and the first reversal indicated that this effect was likely driven by a generalized learning impairment rather than a specific deficit in reversal learning (Figure S1). Importantly, however, analysis of secondary behavioral measures, including choice and reward latencies (Figures S2, S3) and the number of completed trials (Figure S4), suggest that these findings were not driven by a nonspecific disruption in the ability or desire to complete the task. Overall, these results indicate that the PCP-induced PRL deficit was likely mediated by vmOFC hyperactivity and that inhibition of vmOFC glutamate cell activity ameliorated this performance deficit.

Analysis of win-stay responding (Figure 2A) showed that as testing progressed, the propensity to repeat rewarded responses increased in both treatment groups ($F_{19,1862} = 168.28$, $p < .001$) (Figure 2B). However, a significant treatment × opsin interaction also emerged ($F_{2,98} = 6.19$, $p < .01$). As shown in Figure 2C and similar to the data on the number of completed reversals, this interaction reflected 1) a PCP-induced reduction in YFP-expressing rats, 2) a reduction in saline-treated rats when vmOFC glutamate cells were activated with ChR2, and 3) rescue of the PCP-induced deficit when vmOFC glutamate cell activity was inhibited with halo. A treatment × day interaction ($F_{2,98} = 1.75$, $p < .05$) was due to a PCP-induced reduction in win-stay responses on days 10 and 12 ($p < .05$).

Analysis of lose-shift responses (Figure 3A) also revealed a main effect of day ($F_{19,1862} = 30.45$, $p < .001$), indicating that the propensity to switch responses after nonrewarded outcomes increased modestly with training (Figure 3B). A main effect of treatment ($F_{1,98} = 5.34$, $p < .05$) and sex ($F_{1,98} = 10.38$, $p < .01$) revealed that lose-shift responding was lower in PCP-treated rats ($p < .05$) and female rats ($p < .01$). A main effect of opsin ($F_{2,98} = 5.06$, $p < .01$) was also evident. Compared with YFP-expressing rats, lose-shift responding was reduced in ChR2-expressing rats ($p < .05$) but not in halo-expressing rats ($p > .79$) (Figure 3C). No interaction terms were significant (all Fs < 2.75). Collectively, these data suggest that the PCP-induced impairment in PRL was predominantly mediated by reduced reward sensitivity, and this deficit was rescued by inhibiting vmOFC glutamate cell activity. This conclusion was supported by logistic regression analysis (Figure S5).

We fit 2 Q-learning computational models to the data to further explore the behavioral mechanisms underlying these effects. Comparison of the Bayesian information criterion revealed that the model with the single learning rate was a better fit for our dataset than the model with separate learning rates for wins versus losses (329.43 vs. 332.82, respectively). The effects of our experimental manipulation on the parameters for the two-alpha forget model are shown in Figure S6.

The best-fitting model included 3 free parameters (learning rate, inverse temperature, and forget rate). In our previous work, this model (Figure 4A) revealed a lower learning rate in PCP-treated rats (38). Here, we found that the learning rate increased as training progressed ($F_{19,1862} = 82.23$, $p < .001$) (Figure 4B–D). In addition, a treatment × opsin interaction was evident ($F_{2,98} = 4.99$, $p < .01$). As shown in Figure 4E and consistent with our previous findings, the learning rate was lower in YFP-expressing rats treated with PCP versus those treated with saline. In addition, in saline-treated rats, we found that activating vmOFC glutamate neurons with ChR2 resulted in lower learning rates than those seen in YFP-expressing saline-treated rats. Perhaps most importantly, when vmOFC glutamate cell activity was inhibited in PCP-treated rats by stimulating halo, the reduction in the learning rate was ameliorated.

We previously showed that the parameters in our Q-learning model are recoverable (38). To validate the application of the model to the current dataset, we performed a posterior predictive check by using the best-fitting model parameters to generate simulated data and then comparing those data to the actual behavior. Figure 4F shows a close match between the rodent and simulated data for each treatment group (saline, PCP) and opsin (YFP, ChR2, halo), confirming that the model captured PRL performance accurately. The PCP-induced alteration in Q-learning was largely restricted to the learning rate. Although the forget parameter was unaffected by treatment, a sex × day interaction was evident (Figure S7). The inverse temperature parameter analysis revealed a significant four-way interaction (Figure S8). However, the differences that mediated this interaction were restricted to the earlier test days.

DISCUSSION

Our findings are consistent with previous work showing that disrupting glutamate transmission during early postnatal neurodevelopment impaired PRL performance. Replicating our previous findings (38), postnatal PCP-treated rats showed reduced win-stay responding and lower learning rates than saline-treated rats. The current study extends these previous efforts by showing that PCP-induced impairments involve disrupted regulation of vmOFC glutamate activity. More specifically, saline-treated rats showed PRL deficits similar to those observed in PCP-treated rats when vmOFC glutamate neurons were hyperactivated (ChR2). Most strikingly, the opposite was also true: we were able to rescue the PCP-induced deficits in PRL by inhibiting vmOFC glutamate activity.

These data indicate that disinhibition or hyperactivation of the vmOFC in postnatal PCP-treated rats may be a core pathophysiological mechanism contributing to impaired PRL. Indeed, previous reports have shown that inhibition of the medial OFC improved reversal learning (42,45) and has been linked to win-stay responding (42,46), whereas we have previously shown that activation of the vmOFC reduced win-stay responding during the PRL task (42). Interestingly, the postnatal PCP-induced disruption in PRL performance seemed to reflect a generalized impairment in learning, disrupting performance in a stage-independent manner. By contrast, optogenetic manipulation of vmOFC activity produced a stage-dependent effect on PRL performance. More specifically, hyperactivation of vmOFC glutamate neurons impaired performance during the initial discrimination, whereas inhibition of vmOFC glutamate cell activity improved PRL performance after the reward contingencies had reversed. Coordination of

pyramidal cell activity (47) and NMDAR signaling (48) within the OFC is critical for reversal learning. Indeed, reversal learning impairments in *Plaur* knockout mice resulted from reduced GABAergic interneuron expression and an elevation in baseline OFC activity (47). Thus, the improvement in performance evident after the contingency reversal is consistent with the notion that inhibition of OFC activity helps facilitate flexible decision making.

Another major outcome of the current study is the reduced learning rate that we observed in postnatal PCP-treated rats. This effect not only replicates our previous finding (38) but is also consistent with another study in which the NMDAR antagonist MK-801 was administered during PRL performance (49). Systemic administration of MK-801 produces a sustained increase in pyramidal cell activity within the OFC (24). Thus, our current findings support the notion that postnatal PCP treatment disrupts the ability to regulate glutamatergic activity within the vmOFC, but that hyperactivation of vmOFC glutamate cell

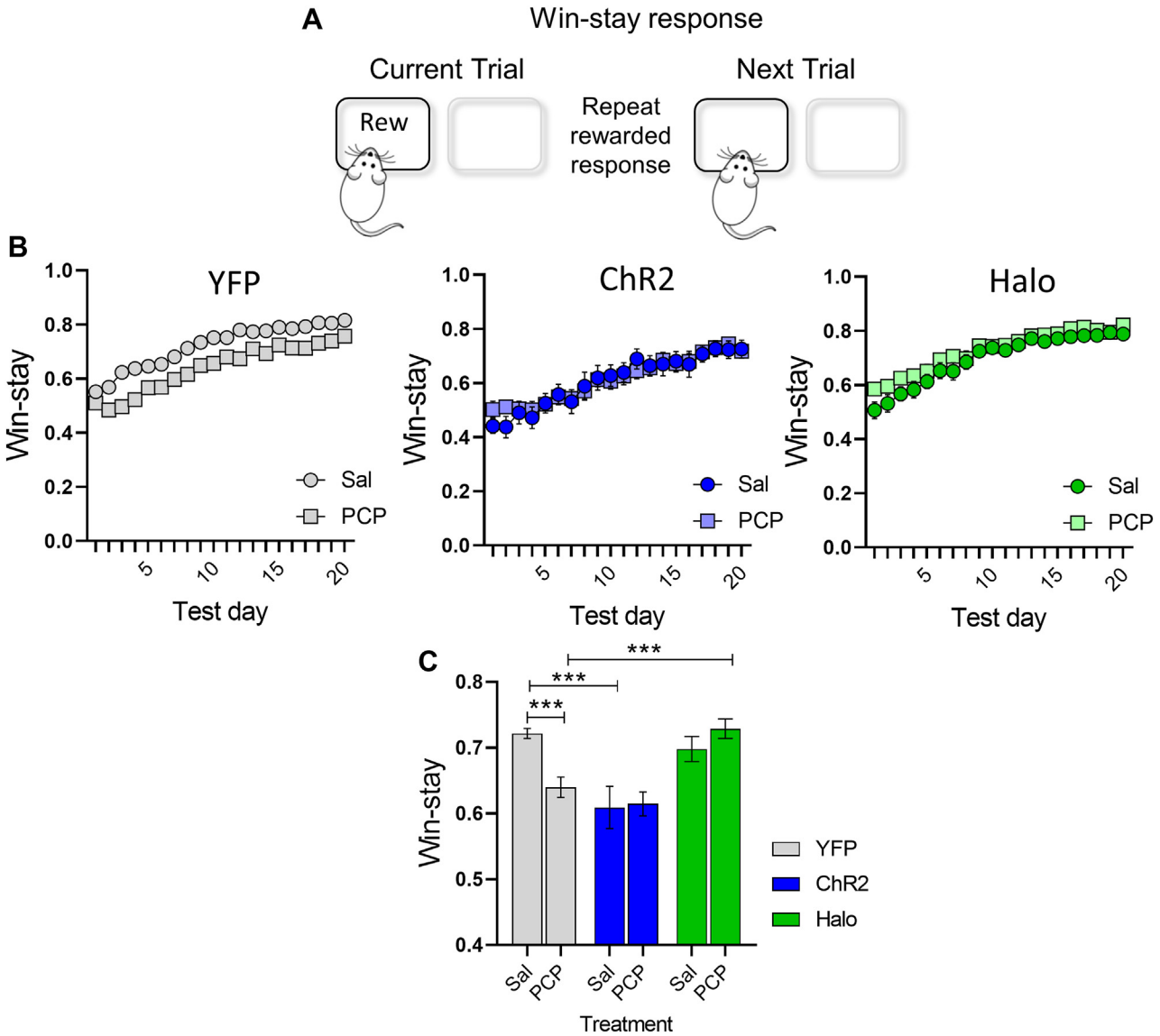

Figure 2. Effect of manipulating ventromedial orbitofrontal cortex glutamate cell activity on win-stay responding. Repeating the same response after a reward was delivered constitutes a win-stay response **(A)**. In both treatment groups (saline, PCP) and 3 opsin groups (YFP, ChR2, halo), win-stay responses increased across the 20-day testing period **(B)**. However, compared with saline-treated rats expressing YFP, win-stay responding was reduced in PCP-treated rats expressing YFP and saline-treated rats expressing ChR2. Compared with PCP-treated rats expressing YFP, win-stay responding was increased in PCP-treated rats expressing halo **(C)**. Circles indicate saline-treated rats. Squares indicate PCP-treated rats. Gray color indicates YFP-expressing rats, blue indicates ChR2-expressing rats, and green indicates halo-expressing rats. Saline YFP, $n = 11$ male, $n = 10$ female; saline ChR2, $n = 7$ male, $n = 8$ female; saline halo, $n = 9$ male, $n = 9$ female; PCP YFP, $n = 11$ male, $n = 10$ female; PCP ChR2, $n = 9$ male, $n = 7$ female; PCP halo, $n = 9$ male, $n = 10$ female. Data are presented as mean ± SEM. ***$p < .001$. ChR2, channelrhodopsin-2; halo, halorhodopsin; PCP, phencyclidine; Sal, saline; YFP, yellow fluorescent protein.

activity leads to an attenuation in the rate at which outcomes update value estimates. The learning rate is critical for trial-to-trial learning (50–53). While slow procedural learning is relatively intact in patients with schizophrenia (54,55), impairments in the ability to make rapid behavioral adjustments in response to the feedback just received are evident (15). Although PRL performance was impaired overall in postnatal PCP-treated rats, their performance improved over the 20-day test period. This finding shows that postnatal PCP-treated rats could learn the task's basic rules. Instead, an impairment in the ability to choose the best action based on recent outcome history likely played a role in their suboptimal performance. Indeed, our logistic regression analysis showed that PCP-treated rats had difficulty using rewarded outcomes from the previous trial to guide subsequent decisions, whereas there was no difference for trials farther back in history. Furthermore, this impairment was induced in saline-treated rats when ChR2 was stimulated to increase neural activity but ameliorated in PCP-treated rats by stimulating halo to inhibit neural activity.

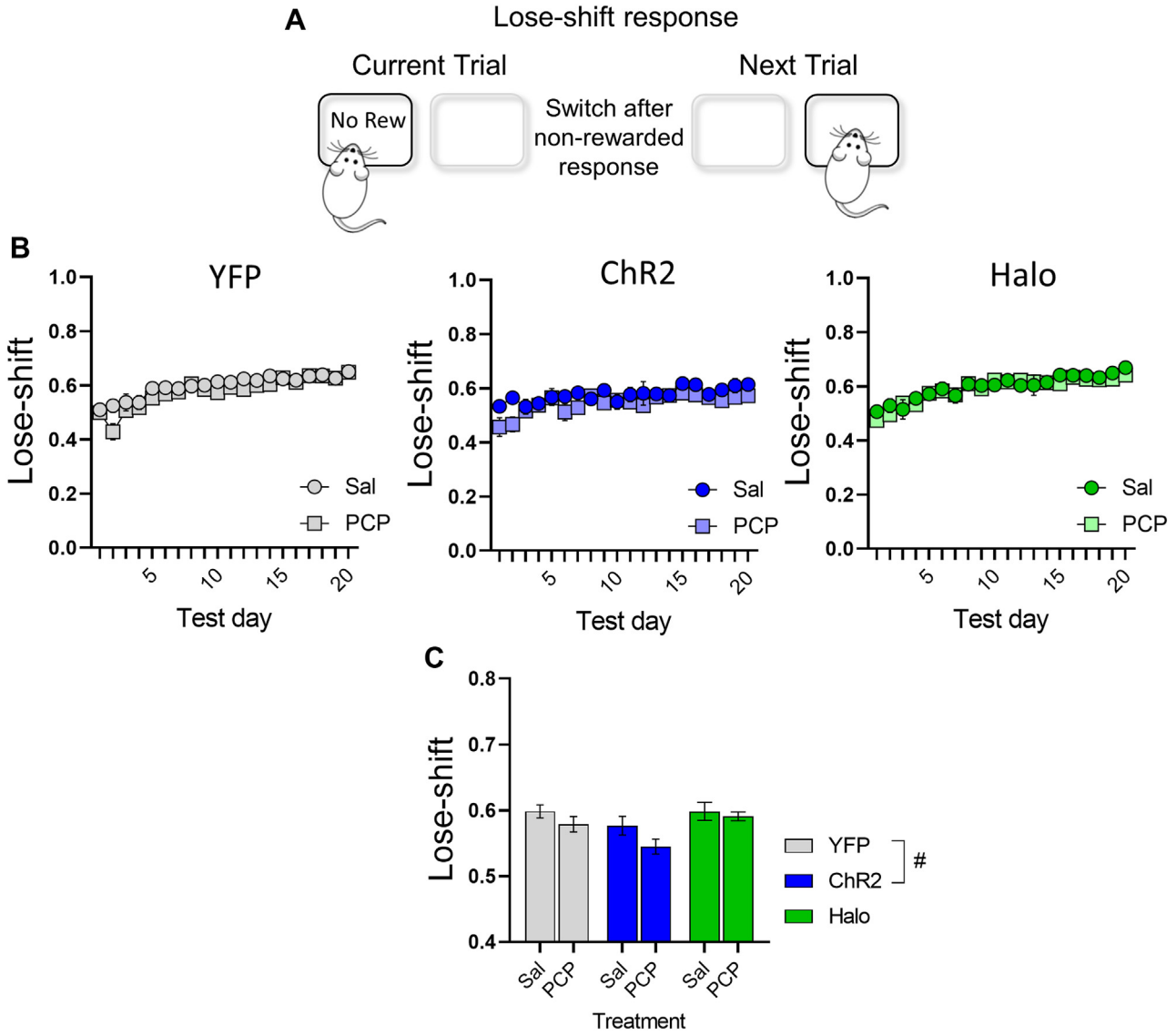

Figure 3. Effect of manipulating ventromedial orbitofrontal cortex glutamate cell activity on lose-shift responses. Switching to the alternative option when the previous response did not yield a reward constitutes a lose-shift response **(A)**. Lose-shift responding was modestly increased in all rats across the 20-day testing period **(B)**. Independent of saline/PCP treatment, lose-shift responding was reduced in rats expressing ChR2 compared with rats expressing YFP **(C)**. Circles indicate saline-treated rats. Squares indicate PCP-treated rats. Gray color indicates YFP-expressing rats, blue indicates ChR2-expressing rats, and green indicates halo-expressing rats. Saline YFP, $n = 11$ male, $n = 10$ female; saline ChR2, $n = 7$ male, $n = 8$ female; saline halo, $n = 9$ male, $n = 9$ female; PCP YFP, $n = 11$ male, $n = 10$ female; PCP ChR2, $n = 9$ male, $n = 7$ female; PCP halo, $n = 9$ male, $n = 10$ female. Data are presented as mean ± SEM. #$p < .05$. ChR2, channelrhodopsin-2; halo, halorhodopsin; PCP, phencyclidine; Rew, reward; Sal, saline; YFP, yellow fluorescent protein.

Thus, in the context of our current findings, the functional hyperactivity of the OFC that has been observed in patients with schizophrenia (24) may disrupt reward sensitivity and the ability to use rewards delivered during the previous trial to guide current choices.

The inclusion of male and female rats in our study revealed several sex differences that warrant discussion. First, male rats completed more trials than female rats (independent of treatment or opsin group). Because female rats are smaller than male rats, this effect may have resulted from satiety (both sexes received 45-mg sucrose pellets) or from male rats being more resilient to the bilateral fiber tethering. Importantly, however, we did not observe any difference in the latency to collect the reward once delivered, thus ruling out differences in motivation to complete the task. We also found that male rats had a higher proportion of lose-shift responses than female rats. Although most studies using the PRL only include male rats, this sex-dependent effect on lose-shift responding is consistent with a recent study (56). Finally, we observed a reduced rate at which the unchosen action value decayed in female rats, an effect that only emerged after several days of testing. While Q-learning models with a forget rate have been used in the past (57,58), no sex differences have been reported for this measure. Indeed, our previous study that used an identical Q-learning model to analyze postnatal PCP-induced deficits in the PRL task did not reveal a sex difference in the forget rate (38). However, because the sex effect was independent of treatment or opsin groups, the statistical analysis collapsed groups, thereby increasing the sample size and likely increasing our ability to detect subtle sex differences on this measure. Importantly, the sex differences that we observed did not affect the major conclusions of our study but nonetheless highlight the importance

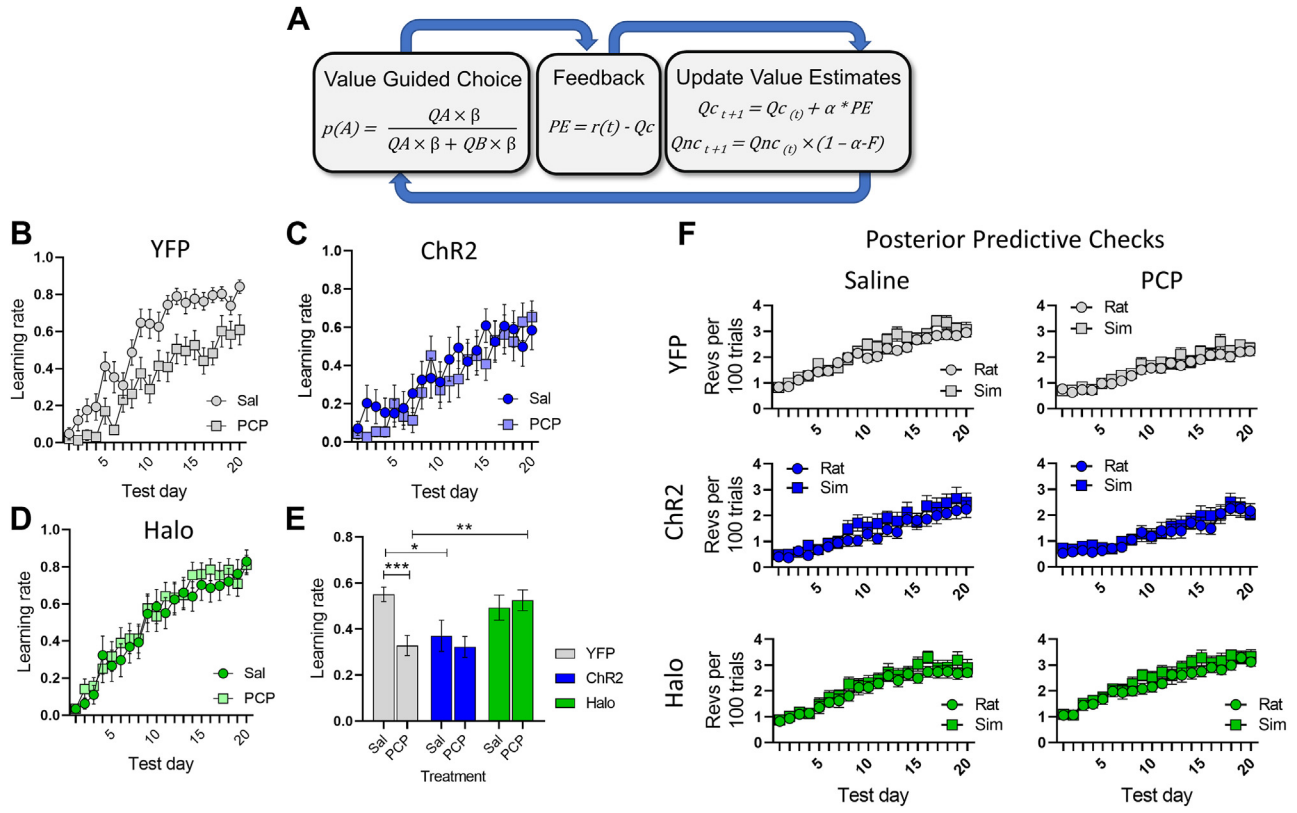

Figure 4. Computational model of reinforcement learning. The Q-learning model that we used to characterize probabilistic reversal learning performance used the softmax equation to convert action value into choice probabilities. The balance between exploratory and exploitative choices is regulated by the inverse temperature (β) parameter. To update value estimates based on the outcome, we first calculated the reward PE by subtracting the expected outcome from the actual outcome received. The rate at which a PE updates the value of the chosen action is controlled by the learning rate (α) parameter. In addition, the unchosen action value was decayed to simulate forgetting. The rate at which the value of the unchosen action decays is controlled by the forget parameter (α-F) **(A)**. In all groups, the learning rate increased throughout the 20-day testing period **(B–D)**. However, compared with saline-treated rats expressing YFP, the learning rate was reduced in PCP-treated rats expressing YFP and saline-treated rats expressing ChR2. Compared with PCP-treated rats expressing YFP, the learning rate was increased in PCP-treated rats expressing halo **(E)**. Circles indicate saline-treated rats. Squares indicate PCP-treated rats. Gray color indicates YFP-expressing rats, blue indicates ChR2-expressing rats, and green indicates halo-expressing rats. We simulated probabilistic reversal learning data using the best-fitting parameter values to validate the model. This posterior predictive check revealed a close match between the simulated (squares) and actual rodent (circles) data in each treatment group (saline, PCP) and opsin group (YFP, ChR2, halo), indicating that the model captured the data well **(F)**. Saline YFP, $n = 11$ male, $n = 10$ female; saline ChR2, $n = 7$ male, $n = 8$ female; saline halo, $n = 9$ male, $n = 9$ female; PCP YFP, $n = 11$ male, $n = 10$ female; PCP ChR2, $n = 9$ male, $n = 7$ female; PCP halo, $n = 9$ male, $n = 10$ female. Data are presented as mean ± SEM. *$p < .05$, **$p < .01$, ***$p < .001$. ChR2, channelrhodopsin-2; halo, halorhodopsin; PCP, phencyclidine; PE, prediction error; Revs, reversals; Sal, saline; sim, simulated; YFP, yellow fluorescent protein.

of including both male and female rats in behavioral neuroscience studies.

Blockade of NMDAR neurotransmission in rodents during early postnatal neurodevelopment produces several neuropathological changes that persist throughout adulthood (30,59) and are reminiscent of deficits observed in patients with schizophrenia (20,21,60–62). These include a reduction in dendritic spine density of cortical pyramidal neurons (63), alterations in NMDAR subunit composition or expression (64–66), and disruptions in synaptic plasticity (67). Perhaps most importantly, however, is that several reports have shown that postnatal PCP treatment induces long-lasting impairments in parvalbumin-positive GABAergic interneurons within the prefrontal cortex, thereby reducing the frequency of miniature inhibitory postsynaptic currents leading to disinhibition of cortical pyramidal cells (39,40,63). Indeed, our findings suggest that hyperactivity of vmOFC glutamate neurons may represent a core pathophysiological mechanism underlying the PRL impairments observed in postnatal PCP-treated rats. Although it has been shown that parvalbumin-positive GABAergic interneurons within the OFC are critical for reversal learning (47), we targeted glutamatergic neurons because our previous work had shown that suppression of vmOFC glutamate cell activity occurs during reward consumption, and vmOFC activation impaired PRL by reducing reward sensitivity (42). However, because parvalbumin-positive GABAergic interneurons play a crucial role in regulating glutamatergic neuron activity (19,68), it is tempting to speculate that PCP-induced impairments in PRL would also be ameliorated by enhancing vmOFC GABAergic activity (rather than inhibiting glutamate activity as in the current study). With the recent development of transgenic rats expressing cre-recombinase in parvalbumin-positive GABAergic interneurons (69–71), this hypothesis could be tested in future investigations by using cre-dependent ChR2 expression and increasing GABAergic activity within the vmOFC of PCP-treated rats. In addition, some OFC neurons respond to reward, whereas others do not (51,72). This heterogeneity may reflect distinct populations of cortical neurons that project to different downstream targets (73), but the current study would have manipulated the activity of any transfected neurons that received optical stimulation. Importantly, the vmOFC sends glutamatergic projections to multiple brains regions that are also implicated in reward learning and decision making, such as the amygdala and striatum (74,75). Interestingly, ablation of the striatum disrupts reversal learning (76,77) and the formation of attentional sets (78). Therefore, in addition to targeting inhibitory neurons within the vmOFC, future research that targets the vmOFC glutamatergic projections to the striatum would further delineate the role of aberrant OFC excitatory activity and maladaptive decision making.

Conclusions

In conclusion, the current investigation demonstrated that postnatal PCP treatment impaired PRL performance by reducing reward sensitivity and lowering the learning rate. Furthermore, these data demonstrated that hyperactivation of vmOFC glutamate neurons induced impairments in saline-treated rats that resembled those observed in PCP-treated rats. Most importantly, inhibiting vmOFC glutamate neurons rescued PCP-induced deficits in PRL performance. Thus, our findings support the hypothesis that pharmacological or neuromodulatory strategies aimed at normalizing vmOFC activity represent a potential therapeutic target for disrupted cognitive flexibility in adults with schizophrenia.

ACKNOWLEDGMENTS AND DISCLOSURES

This work was supported by the National Institute of Mental Health (Grant No. R01MH108653 [to SAB] and Grant No. R01MH111676 [to DGD]) and a Veterans Affairs Merit Award (Award No. I01 BX005209 [to SBP]).

SAB designed and ran the experiments, analyzed the data, and was the primary writer of the manuscript. MMT assisted with running the experiments and with writing the manuscript. MMT and LF conducted the immunohistochemistry procedure; TSH and SBP assisted with writing the manuscript; and DGD assisted with implementing the Q-learning analysis and writing the manuscript.

The authors report no biomedical financial interests or potential conflicts of interest.

ARTICLE INFORMATION

From the Department of Psychiatry, University of California San Diego, La Jolla, California (MMT, SBP, SAB); Research Service, VA San Diego Healthcare System, La Jolla, California (MMT, TSH, SBP, SAB); Department of Neurosciences, University of California San Diego, La Jolla, California (LF, TSH); Center for Depression, Anxiety and Stress Research, McLean Hospital, Belmont, Massachusetts (DGD); and Harvard Medical School, Boston, Massachusetts (DGD).

Address correspondence to Samuel A. Barnes, Ph.D., at sabarnes@ucsd.edu.

Received Apr 12, 2023; revised Jul 12, 2023; accepted Aug 1, 2023.

Supplementary material cited in this article is available online at https://doi.org/10.1016/j.bpsgos.2023.08.002.

REFERENCES

1. Culbreth AJ, Gold JM, Cools R, Barch DM (2016): Impaired activation in cognitive control regions predicts reversal learning in schizophrenia. Schizophr Bull 42:484–493.
2. Reddy LF, Waltz JA, Green MF, Wynn JK, Horan WP (2016): Probabilistic reversal learning in schizophrenia: Stability of deficits and potential causal mechanisms. Schizophr Bull 42:942–951.
3. Schlagenhauf F, Huys QJM, Deserno L, Rapp MA, Beck A, Heinze HJ, *et al.* (2014): Striatal dysfunction during reversal learning in unmedicated schizophrenia patients. NeuroImage 89:171–180.
4. Tezcan D, Tumkaya S, Bora E (2017): Reversal learning in patients with obsessive–compulsive disorder (OCD) and their unaffected relatives: Is orbitofrontal dysfunction an endophenotype of OCD? Psychiatry Res 252:231–233.
5. Pilhatsch M, Pooseh S, Junke A, Kohno M, Petzold J, Sauer C, Smolka MN (2020): Probabilistic reversal learning deficits in patients with methamphetamine use disorder-A longitudinal pilot study. Front Psychiatry 11:588768.
6. Cools R, Altamirano L, D'Esposito M (2006): Reversal learning in Parkinson's disease depends on medication status and outcome valence. Neuropsychologia 44:1663–1673.
7. Robinson OJ, Chase HW (2017): Learning and choice in mood disorders: Searching for the computational parameters of anhedonia. Comput Psychiatr 1:208–233.
8. Strauss GP, Thaler NS, Matveeva TM, Vogel SJ, Sutton GP, Lee BG, Allen DN (2015): Predicting psychosis across diagnostic boundaries: Behavioral and computational modeling evidence for impaired reinforcement learning in schizophrenia and bipolar disorder with a history of psychosis. J Abnorm Psychol 124:697–708.
9. Cáceda R, Nemeroff CB, Harvey PD (2014): Toward an understanding of decision making in severe mental illness. J Neuropsychiatry Clin Neurosci 26:196–213.

10. Barnes SA, Der-Avakian A, Young JW (2017): Preclinical models to investigate mechanisms of negative symptoms in schizophrenia. Schizophr Bull 43:706–711.
11. Izquierdo A, Brigman JL, Radke AK, Rudebeck PH, Holmes A (2017): The neural basis of reversal learning: An updated perspective. Neuroscience 345:12–26.
12. Bari A, Theobald DE, Caprioli D, Mar AC, Aidoo-Micah A, Dalley JW, Robbins TW (2010): Serotonin modulates sensitivity to reward and negative feedback in a probabilistic reversal learning task in rats. Neuropsychopharmacology 35:1290–1301.
13. Sanchez-Roige S, Barnes SA, Mallari J, Wood R, Polesskaya O, Palmer AA (2022): A mutant allele of glycoprotein M6-B (Gpm6b) facilitates behavioral flexibility but increases delay discounting. Genes Brain Behav 21:e12800.
14. Waltz JA, Kasanova Z, Ross TJ, Salmeron BJ, McMahon RP, Gold JM, Stein EA (2013): The roles of reward, default, and executive control networks in set-shifting impairments in schizophrenia. PLOS ONE 8: e57257.
15. Strauss GP, Waltz JA, Gold JM (2013): A review of reward processing and motivational impairment in schizophrenia. Schizophr Bull 40(suppl 2):S107–S116.
16. Nakamura M, Nestor PG, Levitt JJ, Cohen AS, Kawashima T, Shenton ME, McCarley RW (2008): Orbitofrontal volume deficit in schizophrenia and thought disorder. Brain 131:180–195.
17. Whitfield-Gabrieli S, Thermenos HW, Milanovic S, Tsuang MT, Faraone SV, McCarley RW, *et al.* (2009): Hyperactivity and hyperconnectivity of the default network in schizophrenia and in first-degree relatives of persons with schizophrenia. Proc Natl Acad Sci U S A 106:1279–1284.
18. Zheng J, Zhang Y, Guo X, Duan X, Zhang J, Zhao J, Chen H (2016): Disrupted amplitude of low-frequency fluctuations in antipsychotic-naïve adolescents with early-onset schizophrenia. Psychiatry Res Neuroimaging 249:20–26.
19. Gonzalez-Burgos G, Lewis DA (2012): NMDA receptor hypofunction, parvalbumin-positive neurons, and cortical gamma oscillations in schizophrenia. Schizophr Bull 38:950–957.
20. Lewis DA, Curley AA, Glausier JR, Volk DW (2012): Cortical parvalbumin interneurons and cognitive dysfunction in schizophrenia. Trends Neurosci 35:57–67.
21. Reynolds GP, Abdul-Monim Z, Neill JC, Zhang ZJ (2004): Calcium binding protein markers of GABA deficits in schizophrenia—Postmortem studies and animal models. Neurotox Res 6:57–61.
22. Markram H, Toledo-Rodriguez M, Wang Y, Gupta A, Silberberg G, Wu C (2004): Interneurons of the neocortical inhibitory system. Nat Rev Neurosci 5:793–807.
23. Toader O, von Heimendahl M, Schuelert N, Nissen W, Rosenbrock H (2020): Suppression of parvalbumin interneuron activity in the prefrontal cortex recapitulates features of impaired excitatory/inhibitory balance and sensory processing in schizophrenia. Schizophr Bull 46:981–989.
24. Homayoun H, Moghaddam B (2008): Orbitofrontal cortex neurons as a common target for classic and glutamatergic antipsychotic drugs. Proc Natl Acad Sci U S A 105:18041–18046.
25. Tan HY, Sust S, Buckholtz JW, Mattay VS, Meyer-Lindenberg A, Egan MF, *et al.* (2006): Dysfunctional prefrontal regional specialization and compensation in schizophrenia. Am J Psychiatry 163:1969–1977.
26. Ragland JD, Gur RC, Valdez J, Turetsky BI, Elliott M, Kohler C, *et al.* (2004): Event-related fMRI of frontotemporal activity during word encoding and recognition in schizophrenia. Am J Psychiatry 161:1004–1015.
27. Fatemi SH, Folsom TD (2009): The neurodevelopmental hypothesis of schizophrenia, revisited. Schizophr Bull 35:528–548.
28. Rapoport JL, Giedd JN, Gogtay N (2012): Neurodevelopmental model of schizophrenia: Update 2012. Mol Psychiatry 17:1228–1238.
29. Weickert CS, Fung SJ, Catts VS, Schofield PR, Allen KM, Moore LT, *et al.* (2013): Molecular evidence of N-methyl-D-aspartate receptor hypofunction in schizophrenia. Mol Psychiatry 18:1185–1192.
30. Grayson B, Barnes SA, Markou A, Piercy C, Podda G, Neill JC (2016): Postnatal phencyclidine (PCP) as a neurodevelopmental animal model of schizophrenia pathophysiology and symptomatology: A review. Curr Top Behav Neurosci 29:403–428.
31. Powell SB (2010): Models of neurodevelopmental abnormalities in schizophrenia. Curr Top Behav Neurosci 4:435–481.
32. Cope ZA, Powell SB, Young JW (2016): Modeling neurodevelopmental cognitive deficits in tasks with cross-species translational validity. Genes Brain Behav 15:27–44.
33. Broberg BV, Dias R, Glenthøj BY, Olsen CK (2008): Evaluation of a neurodevelopmental model of schizophrenia—Early postnatal PCP treatment in attentional set-shifting. Behav Brain Res 190:160–163.
34. Broberg BV, Glenthøj BY, Dias R, Larsen DB, Olsen CK (2009): Reversal of cognitive deficits by an ampakine (CX516) and sertindole in two animal models of schizophrenia—Sub-chronic and early postnatal PCP treatment in attentional set-shifting. Psychopharmacol (Berl) 206:631–640.
35. Terranova JP, Chabot C, Barnouin MC, Perrault G, Depoortere R, Griebel G, Scatton B (2005): SSR181507, a dopamine D(2) receptor antagonist and 5-HT(1A) receptor agonist, alleviates disturbances of novelty discrimination in a social context in rats, a putative model of selective attention deficit. Psychopharmacol (Berl) 181:134–144.
36. Secher T, Berezin V, Bock E, Glenthøj B (2009): Effect of an NCAM mimetic peptide FGL on impairment in spatial learning and memory after neonatal phencyclidine treatment in rats. Behav Brain Res 199:288–297.
37. Wang C, McInnis J, Ross-Sanchez M, Shinnick-Gallagher P, Wiley JL, Johnson KM (2001): Long-term behavioral and neurodegenerative effects of perinatal phencyclidine administration: Implications for schizophrenia. Neuroscience 107:535–550.
38. Tranter MM, Aggarwal S, Young JW, Dillon DG, Barnes SA (2023): Reinforcement learning deficits exhibited by postnatal PCP-treated rats enable deep neural network classification. Neuropsychopharmacology 48:1377–1385.
39. Kaalund SS, Riise J, Broberg BV, Fabricius K, Karlsen AS, Secher T, *et al.* (2013): Differential expression of parvalbumin in neonatal phencyclidine-treated rats and socially isolated rats. J Neurochem 124:548–557.
40. Kjaerby C, Broberg BV, Kristiansen U, Dalby NO (2014): Impaired GABAergic inhibition in the prefrontal cortex of early postnatal phencyclidine (PCP)-treated rats. Cereb Cortex 24:2522–2532.
41. Kjaerby C, Bundgaard C, Fejgin K, Kristiansen U, Dalby NO (2013): Repeated potentiation of the metabotropic glutamate receptor 5 and the alpha 7 nicotinic acetylcholine receptor modulates behavioural and GABAergic deficits induced by early postnatal phencyclidine (PCP) treatment. Neuropharmacology 72:157–168.
42. Barnes SA, Dillon DG, Young JW, Thomas ML, Faget L, Yoo JH, *et al.* (2023): Modulation of ventromedial orbitofrontal cortical glutamatergic activity affects the explore-exploit balance and influences value-based decision-making. Cereb Cortex 33:5783–5796.
43. Broberg BV, Madsen KH, Plath N, Olsen CK, Glenthøj BY, Paulson OB, *et al.* (2013): A schizophrenia rat model induced by early postnatal phencyclidine treatment and characterized by magnetic resonance imaging. Behav Brain Res 250:1–8.
44. Wilson RC, Collins AGE (2019): Ten simple rules for the computational modeling of behavioral data. eLife 8:e49547.
45. Hervig ME, Fiddian L, Piilgaard L, Božič T, Blanco-Pozo M, Knudsen C, *et al.* (2020): Dissociable and paradoxical roles of rat medial and lateral orbitofrontal cortex in visual serial reversal learning. Cereb Cortex 30:1016–1029.
46. Stopper CM, Green EB, Floresco SB (2014): Selective involvement by the medial orbitofrontal cortex in biasing risky, but not impulsive, choice. Cereb Cortex 24:154–162.
47. Bissonette GB, Schoenbaum G, Roesch MR, Powell EM (2015): Interneurons are necessary for coordinated activity during reversal learning in orbitofrontal cortex. Biol Psychiatry 77:454–464.
48. Bohn I, Giertler C, Hauber W (2003): NMDA receptors in the rat orbital prefrontal cortex are involved in guidance of instrumental behaviour under reversal conditions. Cereb Cortex 13:968–976.

49. Latuske P, von Heimendahl M, Deiana S, Wotjak CT, du Hoffmann J (2022): Sustained MK-801 induced deficit in a novel probabilistic reversal learning task. Front Pharmacol 13:898548.
50. Zha R, Li P, Liu Y, Alarefi A, Zhang X, Li J (2022): The orbitofrontal cortex represents advantageous choice in the Iowa gambling task. Hum Brain Mapp 43:3840–3856.
51. Chase HW, Kumar P, Eickhoff SB, Dombrovski AY (2015): Reinforcement learning models and their neural correlates: An activation likelihood estimation meta-analysis. Cogn Affect Behav Neurosci 15:435–459.
52. K Namboodiri VMK, Hobbs T, Trujillo-Pisanty I, Simon RC, Gray MM, Stuber GD (2021): Relative salience signaling within a thalamo-orbitofrontal circuit governs learning rate. Curr Biol 31:5176–5191.e5.
53. Liu D, Deng J, Zhang Z, Zhang ZY, Sun YG, Yang T, Yao H (2020): Orbitofrontal control of visual cortex gain promotes visual associative learning. Nat Commun 11:2784.
54. Green MF, Kern RS, Williams O, McGurk S, Kee K (1997): Procedural learning in schizophrenia: Evidence from serial reaction time. Cogn Neuropsychiatry 2:123–134.
55. Gold JM, Hahn B, Strauss GP, Waltz JA (2009): Turning it upside down: Areas of preserved cognitive function in schizophrenia. Neuropsychol Rev 19:294–311.
56. Harris C, Aguirre C, Kolli S, Das K, Izquierdo A, Soltani A (2021): Unique features of stimulus-based probabilistic reversal learning. Behav Neurosci 135:550–570.
57. Hattori R, Danskin B, Babic Z, Mlynaryk N, Komiyama T (2019): Area-specificity and plasticity of history-dependent value coding during learning. Cell 177:1858–1872.e15.
58. Ito M, Doya K (2009): Validation of decision-making models and analysis of decision variables in the rat basal ganglia. J Neurosci 29:9861–9874.
59. Mouri A, Noda Y, Enomoto T, Nabeshima T (2007): Phencyclidine animal models of schizophrenia: Approaches from abnormality of glutamatergic neurotransmission and neurodevelopment. Neurochem Int 51:173–184.
60. Akbarian S, Sucher NJ, Bradley D, Tafazzoli A, Trinh D, Hetrick WP, *et al.* (1996): Selective alterations in gene expression for NMDA receptor subunits in prefrontal cortex of schizophrenics. J Neurosci 16:19–30.
61. Forsyth JK, Lewis DA (2017): Mapping the consequences of impaired synaptic plasticity in schizophrenia through development: An integrative model for diverse clinical features. Trends Cogn Sci 21:760–778.
62. Glantz LA, Lewis DA (2000): Decreased dendritic spine density on prefrontal cortical pyramidal neurons in schizophrenia. Arch Gen Psychiatry 57:65–73.
63. Nakatani-Pawlak A, Yamaguchi K, Tatsumi Y, Mizoguchi H, Yoneda Y (2009): Neonatal phencyclidine treatment in mice induces behavioral, histological and neurochemical abnormalities in adulthood. Biol Pharm Bull 32:1576–1583.
64. Sircar R, Follesa P, Ticku MK (1996): Postnatal phencyclidine treatment differentially regulates N-methyl-d-aspartate receptor subunit mRNA expression in developing rat cerebral cortex. Brain Res Mol Brain Res 40:214–220.
65. Sircar R (2003): Postnatal phencyclidine-induced deficit in adult water maze performance is associated with N-methyl-D-aspartate receptor upregulation. Int J Dev Neurosci 21:159–167.
66. Anastasio NC, Johnson KM (2008): Differential regulation of the NMDA receptor by acute and sub-chronic phencyclidine administration in the developing rat. J Neurochem 104:1210–1218.
67. Golitabari N, Mohammadian F, Salari AA, Amani M (2022): Neonatal NMDA blockade alters the LTP, Ltd and cognitive functions in male and female Wistar rats. Neuropharmacology 205:108896.
68. Lee JH, Durand R, Gradinaru V, Zhang F, Goshen I, Kim DS, *et al.* (2010): Global and local fMRI signals driven by neurons defined optogenetically by type and wiring. Nature 465:788–792.
69. Wright AM, Zapata A, Hoffman AF, Necarsulmer JC, Coke LM, Svarcbahs R, *et al.* (2021): Effects of withdrawal from cocaine self-administration on rat orbitofrontal cortex parvalbumin neurons expressing Cre recombinase: sex-dependent changes in neuronal function and unaltered serotonin signaling. eNeuro 8:ENEURO.0017-21.2021.
70. Prasad AA, Xie C, Chaichim C, Nguyen JH, McClusky HE, Killcross S, *et al.* (2020): Complementary roles for ventral pallidum cell types and their projections in relapse. J Neurosci 40:880–893.
71. López-Madrona VJ, Pérez-Montoyo E, Álvarez-Salvado E, Moratal D, Herreras O, Pereda E, *et al.* (2020): Different theta frameworks coexist in the rat hippocampus and are coordinated during memory-guided and novelty tasks. eLife 9:e57313.
72. Rolls ET, Cheng W, Feng J (2020): The orbitofrontal cortex: Reward, emotion and depression. Brain Commun 2:fcaa196.
73. Hernandez JS, Moorman DE (2020): Orbitofrontal cortex encodes preference for alcohol. eNeuro 7:ENEURO.0402-19.2020.
74. Schilman EA, Uylings HB, Galis-de Graaf Y, Joel D, Groenewegen HJ (2008): The orbital cortex in rats topographically projects to central parts of the caudate-putamen complex. Neurosci Lett 432:40–45.
75. Lichtenberg NT, Sepe-Forrest L, Pennington ZT, Lamparelli AC, Greenfield VY, Wassum KM (2021): The medial orbitofrontal cortex-basolateral amygdala circuit regulates the influence of reward cues on adaptive behavior and choice. J Neurosci 41:7267–7277.
76. Castañé A, Theobald DEH, Robbins TW (2010): Selective lesions of the dorsomedial striatum impair serial spatial reversal learning in rats. Behav Brain Res 210:74–83.
77. Cole S, Stone AD, Petrovich GD (2017): The dorsomedial striatum mediates Pavlovian appetitive conditioning and food consumption. Behav Neurosci 131:447–453.
78. Lindgren HS, Wickens R, Tait DS, Brown VJ, Dunnett SB (2013): Lesions of the dorsomedial striatum impair formation of attentional set in rats. Neuropharmacology 71:148–153.